GIS ANALYSIS OF INTEGRATED LANDSAT-TM, TOPOGRAPHIC, GEOLOGIC AND GEOPHYSICAL DATA SETS OF THE BASEMENT AREA OF THE RED SEA HILLS, SUDAN

Franz K. List & Norbert Ott

Freie Universität Berlin, Institute of Geology, Geophysics und Geoinformatics, Berlin, Germany

Commission VII, Working Group 4

KEY WORDS: Geology, Landsat, Integration, GIS, Classification

ABSTRACT

Improved visualization and classification of lithologic units based on multispectral data is of major concern to geologists working with remotely sensed data. The results of spectral digital image analysis of data from current remote sensing systems are often disappointing due to the few and rather wide spectral bands available. Imaging spectrometry (e.g. AVIRIS, GERIS, HYDICE, AMSS) offers a solution for this problem, but hyperspectral data are still scarce and rarely available for the actual area of interest. Another solution is to use additional data sets together with the multispectral data, from existing geologic knowledge to geophysical and gechemical data. Classification of these disparate data sets is then performed in a GIS environment allowing to integrate different data types for improved lithologic discrimination. This approach is similar to the way in which a geologist, without help from a computer, would try to make sense out of the data available to him. Improved visualization of data is another topic with the human interpreter in mind, where data are arranged in a way analogous to our visual perception of the "real world". Examples from the Red Sea Hills, Sudan, serve to illustrate these points.

KURZFASSUNG

Eine Verbesserung der Visualisierung und Klassifizierung geologischer Einheiten auf der Basis multispektraler Daten ist für Geologen, die mit Fernerkundsdaten arbeiten, von großer Bedeutung. Die Ergebnisse spektraler digitaler Bildanalyse von Datensätzen üblicher Fernerkundungssysteme sind aufgrund der wenigen und sehr breitbandigen verfügbaren Spektralkanäle oft enttäuschend. Abhilfe bieten Abbildende Spektrometer wie AVIRIS, GERIS, HYDICE oder AMSS; hyperspektrale Datensätze sind jedoch noch selten und für ein bestimmtes Arbeitsgebiet gewöhnlich nicht verfügbar. Einen anderen Lösungsweg stellt die Einbeziehung zusätzlicher Datensätze, von vorhandenem geologischem Wissen (z.B. geologische Karten) bis zu geophysikalischen und geochemischen Geländedaten, dar. Eine Klassifizierung dieser unterschiedlichen Datensätze kann in einer GIS-Umgebung durchgeführt werden, in der verschiedenartige Datentypen miteinander in Beziehung gesetzt werden können. Dieser Weg ist der klassischen Vorgehensweise eines Geologen verwandt, auch ohne Hilfe eines Rechners die verfügbaren Daten synoptisch zu interpretieren. Eine verbesserte Visualisierung geowissenschaftlicher Daten ist eine weitere Technik, durch die mit Hilfe eines Rechners Daten in einer Weise dargestellt werden, die der üblichen visuellen Erfassung unserer Welt durch den menschlichen Beobachter nahe kommt. Beispiele aus den Red Sea Hills, Sudan, belegen diese Aussagen.

1 INTRODUCTION

1.1 GEOLOGIC SETTING

The Red Sea Hills extend from Egypt into Sudan and Eritrea along the Red Sea, forming part of the Precambrian Arabian-Nubian Shield. A section of this highly complex basement, situated at the Red Sea coast between 17° and 20° N, was being studied within a research project funded by the Deutsche Forschungsgemeinschaft (SFB 69). The study area consists of several terranes which are divided by NE-SW-trending sutures. It is now generally accepted that this situation points to an island-arc assemblage with a number of ophiolite complexes (Almond et al., 1983; Vail, 1988; Shackleton, 1994). During the Pan-African episode (650-450 Ma) the rocks were metamorphosed under greenschist and amphibolite facies conditions. This series known as "Greenschist Assemblage" was intruded by abundant granitoid rocks,

diorites and gabbros. The Precambrian faults became reactivated during the opening of the Red Sea in Pliocene times and represent block boundaries (Schönfeld, 1977).

Fig. 1 shows a georeferenced image mosaic of that area, produced from 5 Landsat TM frames. For the northeastern part of the mosaic 2 Landsat MSS scenes had to be used since the coastal plain is cloud-covered on all available TM data.

The northern part of the mosaic is composed of low-grade metamorphic volcano-sedimentary and metasedimentary rocks, belonging to the Gebeit terrane. A prominent feature in the mosaic is the NE-SW trending Nakasib suture that is cut and dislocated by the NNW-SSE trending Oko shear zone. The Nakasib suture separates the Gebeit terrane from the Haya terran to the south. The metamorphism of the metavolcanics and amphibolite/marble series is higher than that of the Gebeit terrane. A second NE-SW

425

International Archives of Photogrammetry and Remote Sensing. Vol. XXXI, Part B7. Vienna 1996
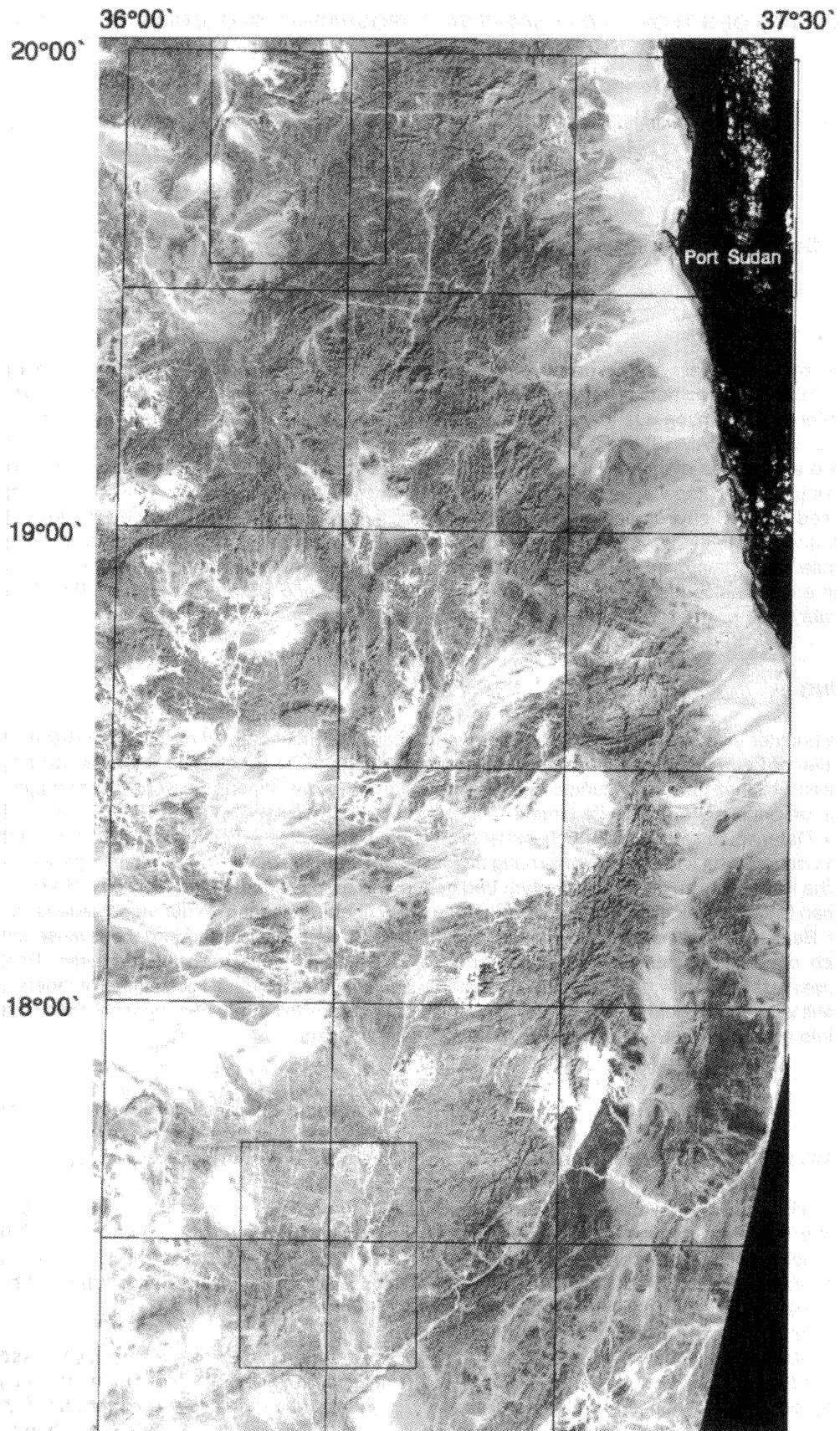
Fig. 1: Georeferenced Landsat image mosaic (original in color) of the Red Sea Hills in Sudan from 17 to 20° N and 36 to 37.30° E (after OTT, 1996). For explanation see text.

426

International Archives of Photogrammetry and Remote Sensing. Vol. XXXI, Part B7. Vienna 1996

trending major structure, the Wadi Ashat zone (REISCH-MANN & KRÖNER, 1994), cuts across the Haya terrane in the middle of the mosaic. To the south a large belt of metavolcanics stands out as a dark bow-shaped prominent feature.

1.2 OBJECTIVES

Since the launch of Landsat-1 in 1972 multispectral data have been widely used for the extraction of thematic information in the fields of geology, mineral exploration, land use and many others. This process of information extraction or classification involves several steps. Starting point is our "real world", the object space, from which we proceed into image space and feature space. The classes we want to obtain are defined in a thematic space and have to correspond, in the end, with actual classes in the real world (LIST, 1993). In this rather complex process two divergent techniques are employed: visual interpretation by a trained interpreter or "automated" classification by means of a digital computer.

Visual interpretation is the time-honored approach used in the earth sciences since the appearence of aerial photographs. As of 1938, "photogeology" can be considered as an established operational method both in the US and in Europe (e.g. ANONYMOUS, 1938; HELBLING, 1938, 1948).

Digital classification evolved rapidly after the launch of Landsat-1. Today, a variety of "supervised" and "unsupervised" classification algorithms is available to the researcher, the maximum likelihood classifier being probably the most widely used one. Still, all these classifiers utilize only the spectral properties of the individual pixels in an image. As compared to visual interpretation, this approach sacrifices a lot of information that is available but not used in the classification process. Such information consists of at least some existing information on the geology of the area studied, or geophysical, lithological, stratigraphic and geochemical data, just to name a few. This is one of the reasons why digital classification of multi-spectral data sets produces, in most cases, inferior results in comparison to a visual interpretation by a trained geologist. The other reason lies, of course, in the fact that what is of interest to the geologist is often covered by weathering products, soil, and vegetation, obstructing the identification of lithology.

One possible solution for this predicament is the use of data from imaging spectrometers like AVIRIS, GERIS, HYDICE oder AMSS. These hyperspectral data sets allow precise definition of individual minerals and mineral mixtures that cannot be achieved with the current broad-band multispectral data from systems like Landsat-TM, IRS or SPOT. Unfortunately, hyperspectral data are still scarce and rarely available of the area of interest. Still, the problem of having to work with data that are diluted or altered by interference from surficial material is there.

A different answer to classification problems is provided by the integration of ancillary data in a GIS environment, making use of the "complimentarity between GIS and remote sensing" (WILKINSON, 1996: 85). In this way, important information can be gleaned from the various sources that are also taken into account in the actual thinking and interpretation process, and be used in addition to spectral information from remotely sensed data. In the following, several examples are presented to illustrate these points:

❑ Improved visualization of data by integrating remote sensing, topographic and geophysical data;

❑ A complementary method for the detection of iron anomalies from band ratioing;

❑ Classification of lithologic units in an image processing / GIS environment using ancillary data.

2 IMPROVED VISUALIZATION

Satellite remote sensing data present a more generalized and thus more abstract image of geologic features than larger-scale aerial photographs. They also mostly lack the stereo capability of aerial photography that leads to a model-like rendition of objects that makes it easier for the human interpreter to correlate information contained in the image to the familiar three-dimensional view of natural objects. The difficulties in interpreting satellite data can be alleviated in several ways:

❑ The spectral content of multispectral imagery can be enhanced in order to provide additional information to the interpreter. This can be achieved by decorrelation of the spectral bands and transformation resp. re-transformation of the data in color space (KAUFMANN & SCHWEINFURTH, 1986, 1988; GILLESPIE ET AL., 1986, 1987).

❑ The remotely sensed image can be draped over a DEM and viewed from several positions in space, thus providing an impression that comes close to the human way of perceiving geologically related features in the field. In combination with height exaggeration and superimposing geophysical or other data, the interpretability of the image data is greatly enhanced. Of course, both methods can be combined by draping color-stretched imagery over a DEM (e.g. LIST ET AL., 1992; LIST & SQUYRES, 1996).

A subscene of the image mosaic of fig. 1 is presented in fig. 2. It shows the region of Jibâl Mugrar, situated at the northern edge of the mosaic. An area of about 30 by 27 km at a scale of about 1 : 100,000 is draped over a DEM derived from toposheets, with a vertical exaggeration factor of 4. The prominent range in the northern part of the scene, Jibâl Mugrar, consists of a syn- to late-tectonic calc-alkaline granitic intrusion, surrounded by metamorphic volcano-sedimentary rocks with low relief. The polygons resulting from an integrated image processing / GIS analysis are superimposed on the model. To the east of Jibâl Mugrar the "iron anomaly" described in the following chapter is shown. In this way the precise location of the anomaly is clearly defined in relation to the topographic features.
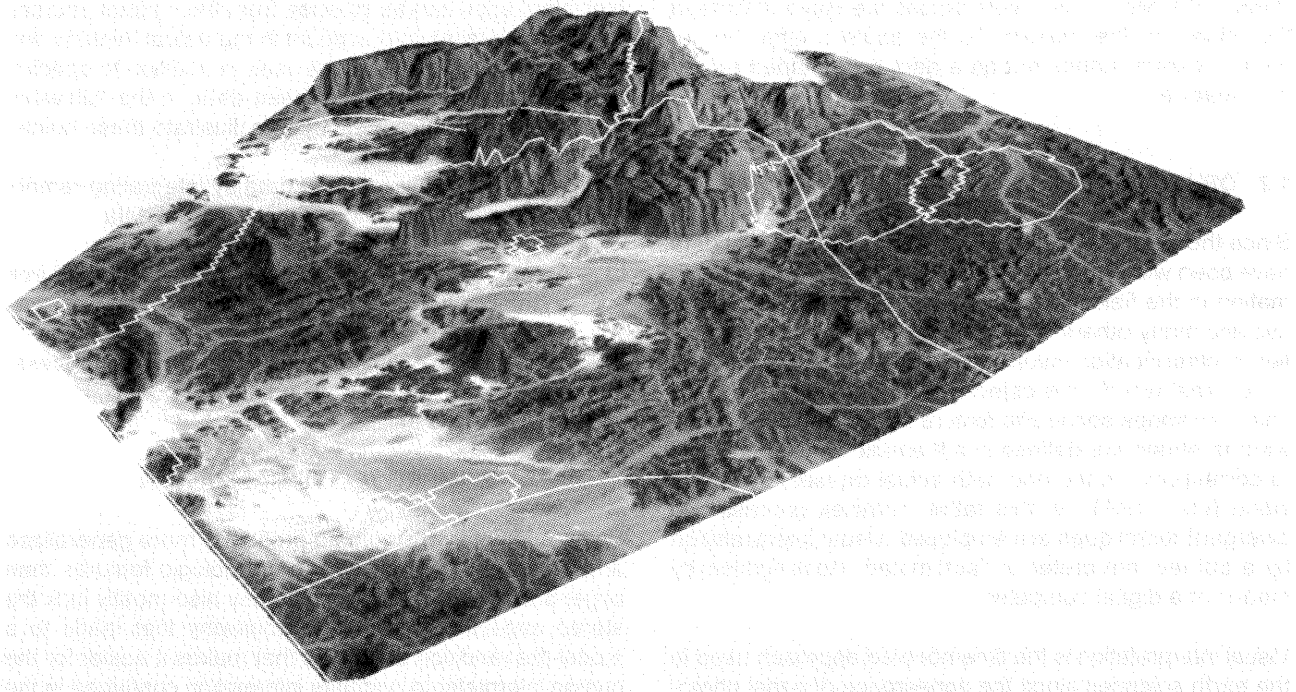
427

International Archives of Photogrammetry and Remote Sensing. Vol. XXXI, Part B7. Vienna 1996

Fig. 2: Spectral band 4 of a Landsat TM mosaic draped over a DEM, showing the area of Jibâl Mugrar. Pixel size as well as DEM cell size is 50 m. Superimposed on the model is the iron anomaly of fig. 4.

3 IRON ANOMALIES

Band ratioing is a powerful method for the enhancement of mineralogical differences seen in multispectral data and their presentation in the form of color ratio images. (ROWAN ET AL., 1974). Landsat TM data are even more suitable for ratioing due to the increased number of significant spectral bands. In geology as well as in mineral exploration, increased iron content of soils or rocks plays an important role. Iron is generally enriched in occurrences of economic minerals that can be thus emphasized in the imagery by the "iron ratio" of TM bands 3/1. Since this ratio is, however, highly sensitive to even small amounts of Fe, it is by no means sure that an iron anomaly in an image is also related to an economically interesting metal occurrence. For instance, quartz sand with a thin coating of limonitic matter will produce a very strong iron anomaly. Two examples of color ratio images are shown in figs. 4 and 6; Ratios 3/1, 5/7 and 3/5 are coded in R, G and B. A 2σ linear stretch and a 2x enhancement of saturation in the IHS color space was applied to the data. Iron enrichment is indicated by reddish hues in the image.

Geophysical data like aeromagnetics or gravity, on the other hand, provide information on larger bodies with increased iron content, also if they are not directly exposed on the surface. As an example, the residuals of aeromagnetic data and gravity residuals of the study area were combined in a GIS. High values of both the magnetic and the gravity residuals suggest the presence of a geologic body with increased iron content. Figs. 5 and 6 show two examples of such anomalies.

In cases where the location of a geophysical anomaly corresponds to a high 3/1 ratio, one can safely assume the existance of a geologic body with increased iron content close to the surface (figs. 2, 3 and 4). On the other hand, if a small-amplitude magnetic and gravity anomaly shows no relatation to an iron signal on the surface (figs. 5 and 6), it can be inferred that there is either a deeper-seated body or that the anomaly is caused by other effects like faults or lithologic changes. (GRANT & WEST, 1965).

4 GIS CLASSIFICATION

Digital classification of multispectral data, when applied to problems of geology, often yields unsatisfactory results due to the low number and wide-band character of the spectral channels. Effects of surficial material further obscure the original lithologic signal. The major drawback of multispectral classification, however, is the fact that pixels are classified individually, without taking into account context and existing a priori knowledge. An integrated image processing/GIS environment allows the scientist to make use of such additional information and to improve the accuracy of digital image classification.

The backbone of a GIS is a relational database in which all map information is archived with reference to a common coordinate system. For the example presented here, bands 1, 4 and 7 (plus the ratios 3/1, 5/7 and 3/5) of five Landsat TM scenes were geo-referenced to a UTM grid and mosaicked, representing an important thematic layer

428

International Archives of Photogrammetry and Remote Sensing. Vol. XXXI, Part B7. Vienna 1996

in the GIS (see fig. 1). Haze and histogram corrections were applied to the data in order to minimize atmospheric influences.

The second data set comprises the available geologic information available for that area. It is contained in a geological map that was produced through a combination of visual image interpretation of "optimized" Landsat TM images (KAUFMANN & SCHWEINFURTH, 1989), field work, and laboratory investigations. The available aeromagnetic and gravity data were also transformed to the UTM grid and input into the GIS.

The geological map of the study area, comprising about 40,000 squ. km, shows 61 geologic/lithologic units. For digital classification as well as for representation on a small-scale map, this number is far too high. Consequently, similar lithologic units were lumped together until 27 major units were left. These units were arranged into 5 groups:

1. Quaternary (3 units);
2. Intrusive rocks (6 units);
3. Sedimentary and metasedimentary rocks (7 units);
4. Volcanic rocks (8 units);
5. Volcano-sedimentary rocks (3 units).

For each group, a mask was created and a maximum likelihood classifier was applied to the ratio data within this mask, using the respective lithologic units as classes. All in all, 240 representative sites (ROIs or AOIs) about which reliable field and petrographic evidence was available were carefully selected within the entire map region and used as "training areas". In this way, both the a priori knowledge from the map and the spectral data could be used in the classification (OTT, 1996). Subsequently, the 5 separate classification results obtained for each of the masked areas were joined for the final classification shown in fig. 7. The classification is presented in its "raw" form, without any smoothing algorithm applied.

The result of a first supervised digital classification using these additional data sets was a significantly improved discrimination of the geologic units as compared to a classification based on spectral data only. Actually, a spectral classification into 27 lithologic classes would be a rather hopeless undertaking in the first place.

The result is also interesting when compared to the original map information used for the masking: There are several cases in which the interpreter was somewhat doubtful about divisions he had made on the map, e.g. the separation of acidic vs. basic intrusives. In this combined classification it can be seen that some of the doubtful decisions were, in fact, not correct.

The resolution of the available geophysical data is, unfortunately, too low to be used in the classification for discriminating most of the individual geologic bodies; only larger structural blocks within the different terranes can be separated. Therefore, the geophysical data sets were not used in the classification. It was also tried to use neural networks for this rather time-consuming process. At the moment, however, the amount of data involved cannot be handled satisfactorily by neural networks.

5 CONCLUSIONS

The combination of image processing and GIS greatly enhances the potential of interpretation and classification of remotely sensed data. The use of GIS technology is a realistic way to include a priori knowledge, topographic, mineralogic and geophysical data sets into the classification process, leading to results superior to both purely spectral classification and existing field/interpretation geological maps.

The combination of topographic and geophysical data with remotely sensed imagery improves the visualization and thus the interpretability of geologic data. GIS classification of geophysical data sets provides a "second opinion" on results of spectral analyses.

6 ACKNOWLEDGEMENTS

7 REFERENCES

ALMOND, D. C., AHMED, F. & DAWOUD, A. S. (1983): Tectonic, metamorphic and magmatic styles in the northern Red Sea Hills of Sudan. - Bull. Fac. Earth Sci., King Abdulaziz Univ., 6, p. 450 - 458, Jeddah.

ANONYMOUS (1938): Aerial photography used extensively in New Guinea oil search. - World Petroleum, 8, 10, p. 44 - 47, Houston, TX.

BOLSTAD, P.V. & LILLESAND, T.M. (1992): Rule-based classification models: flexible integration of satellite imagery and thematic spatial data. - Photogramm. Eng. remote Sens., 58, 7, p. 965 - 971, Bethesda, MD.

GILLESPIE, A. R., KAHLE, A. B. & WALKER, R. E. (1986): Color enhancement of highly correlated images. I. Decorrelation and HSI contrast stretches. - Remote Sens. Envir., 20, p. 209 - 235, New York, NY.

GILLESPIE, A. R., KAHLE, A. B. & WALKER, R. E. (1987): Color enhancement of highly correlated images. II. Channel ratio and "chromaticity" transformation techniques. - Remote Sens. Envir., 22, p. 343 - 365, New York, NY.

GRANT, F. S. & WEST, G. F. (1965): Interpretation theory in applied geophysics. - 584 p., New York (McGraw Hill).

HELBLING, R. (1938): Die Anwendung der Photogrammetrie bei geologischen Kartierungen. - Beitr. geol. Karte Schweiz, N.F., 76, p. 1 - 67, Bern.

HELBLING, R. (1948): Photogeologische Studien im Anschluß an geologische Kartierungen in der Schweiz, insbesondere der Tödikette. - 141 pp., Zürich (Orell Füssli).

429

International Archives of Photogrammetry and Remote Sensing. Vol. XXXI, Part B7. Vienna 1996

HUTCHINSON, C. F. (1982): Techniques for combining Landsat and ancillary data for digital classification improvement. - Photogramm. Eng. remote Sens., **48**, 1, p. 123 - 130, Falls Church, VA.

KAUFMANN, H. (1989): Image processing strategies for mineral exploration in arid areas. - Proceed. Workshop Eartnet Pilot Proj. Landsat TM Appl., Frascati, Italy, December 1987, ESA **SP-1102**, p. 111 - 125, Noordwijk (ESTEC).

KAUFMANN, H. & SCHWEINFURTH, G. (1986): "Spectral maps": Logical consequence of image optimization and digital cartography. - Proceed. 20. internat. Symposium remote Sens. Envir., Nairobi, Kenya, **3**, p. 1423 - 1428, Ann Arbor, MI.

KAUFMANN, H. & SCHWEINFURTH, G. (1988): Definition of processing parameters for TM based "spectral maps" with respect to geologic applications in arid areas. - In: BUCHROITHNER, M. F. & KOSTKA, R., Hrsg.: Remote sensing: Towards operational cartographic applications; Proceed. WILLI NORDBERG Symp. 1987, Graz, Austria, p. 283 - 286, Graz, Austria (Joanneum).

KOCH,W. (1996): Analyse und Visualisierung geowissenschaftlicher Daten mit Hilfe digitaler Bildverarbeitung und eines Geo-Informationssystems.- Beitrag zur regionalen Geologie der Red Sea Hills, Sudan: Geologische Karte, Blatt Port Sudan 1 : 250 000 und Blatt Jebel Hamot 1 : 100 000. - Berliner geowiss. Abhandl. D, 1996 (in preparation).

KOWALIK, W. S. & GLENN, W. E. (1987): Image processing of aeromagnetic data and integration with Landsat images for improved structural interpretation. - Geophysics, **52**, 7, p. 875 - 884, Tulsa, OK.

LIST, F. K. (1993): Use of satellite data for mapping geology and land cover. - In: KONECNY, G., Hrsg.: Workshop and Conference "International Mapping from Space", Working Group IV/2 ISPRS; Schr.-R. IPI, **15**, p. 279 - 286, Hannover.

LIST, F. K., KOCH, W. & SALAHCHOURIAN, M. H. (1992): Geological mapping in arid regions of Africa using satellite imagery - integration of visual and digital techniques. - Internat. Arch. Photogramm. remote Sens., **29**, B4, p. 325 - 332, Washington, DC.

LIST, F. K. & SQUYRES, C. H. (1996): Geologic mapping from satellite data: contribution of remote sensing and GIS technology to hydrocarbon and mineral exploration . - Proceed. 11. them. Conf. geol. remote Sens., Las Vegas, Nevada, **1**, p. 309 - 320, Ann Arbor, MI.

ROWAN, L. C., WETLAUER, P. H., GOETZ, A. F. H., BILLINGSLLEY F. C. & STEWART, J. H. (1974): Discrimination of rock types and detection of hydrothermally altered areas in south-central Nevada by the use of computer-enhanced ERTS images.- U.S. geol. Surv. prof. Pap., **883**, 35 pp., Washington, DC.

SCHÖNFELD, M. (1977): Scherzonen im Kristallin der Red Sea Hills im nordöstlichen Sudan und ihre Bedeutung für die Entwicklung des roten Meeres - erste Ergebnisse einer Auswertung von Landsat-Aufnahmen. - Geotekt. Forsch., **53**, p. 107 - 121, Stuttgart.

SHACKLETON, R. M. (1994): Review of Late Proterozoic sutures, ophiolitic melanges and tectonics of eastern Egypt and north-east Sudan. - Geol. Rundsch., **83**, p. 537 - 546, Stuttgart (Springer).

OTT, N. (1996): GIS-Modellierung und Klassifizierung von geophysikalischen, geologischen und Fernerkundungsdaten aus den südlichen Red Sea Hills (Sudan). - Berliner geowiss. Abhandl. D, 1996 (in preparation).

REISCHMANN, T. & KRÖNER, A. (1992): Late Proterozoic island arc volcanics from Gebeit, Red Sea Hill, north-east Sudan. - Geol. Rundsch., **83**, p. 547 - 563, Stuttgart.

VAIL, J. R. (1988): Tectonics and evolution of the Proterozoic basement of Northeast Africa. - In: EL-GABY, S. & GREILING, R. O. (eds.): The Pan-African Belt of Northeast Africa and adjacent areas, p. 195 - 219, Braunschweig (Vieweg).

WILKINSON, G. G. (1996): A review of current issues in the integration of GIS and remote sensing data. - Int. J. geogr. Inform. Systems, **10**, 1. p. 85 - 101, London.

AUTHORS ADDRESSES

Prof. Dr. Franz K. List
Dipl.-Geol. Norbert Ott
Freie Universität Berlin
Institut für Geologie, Geophysik und Geoinformatik
Malteserstraße 74 - 100
D-12249 Berlin

Tel.: +49 - 30 - 779 2570
Fax: +49 - 30 - 775 2075

430

International Archives of Photogrammetry and Remote Sensing. Vol. XXXI, Part B7. Vienna 1996